

Combined radiation damage, annealing and ageing studies of InGaAsP/InP 1310nm lasers for the CMS Tracker optical links

K. Gill*, R. Grabit, J. Troska, and F. Vasey.
EP Division, CERN.

ABSTRACT

A summary is presented of the combined effects of radiation damage, accelerated annealing and accelerated ageing in 1310nm InGaAsP/InP multi-quantum-well lasers, the type chosen for use in the CMS Tracker optical links. The radiation damage effects are compared for a variety of radiation sources: ^{60}Co -gamma, 0.8MeV (average energy) neutrons, 20MeV (average energy) neutrons and 300MeV/c pions that represent important parts of the spectrum of particles that will be encountered in the CMS Tracker. The relative damage factors of the various sources are calculated by comparing the laser threshold current increase due to radiation damage giving $\sim 0 : 0.12 : 0.53 : 1$ for ^{60}Co -gamma, $\sim 0.8\text{MeV}$ neutrons, $\sim 20\text{MeV}$ neutrons with respect to 300MeV/c pions. The effects of bias current and temperature on the annealing were measured and, in all cases, the annealing is proportional to $\log(\text{annealing time})$. A bias current of 60mA increases the annealing, in terms of the time taken to anneal a given amount, by a factor of 10 relative to 0mA. The annealing rate is also accelerated by heating the irradiated lasers and recovery occurs ~ 10 times faster at 60°C than at 20°C . The long-term ageing properties of irradiated lasers were also measured in an accelerated test carried out at 80°C , for 2500 hours, at a bias current of 60mA. No wearout-related degradation was observed in any of the devices. The combined results of these studies have been used to estimate the long-term damage expected for this type of laser operating inside the CMS Tracker. In the worst case of a laser operating at a distance of 22cm from the beam-axis in the forward region of the Tracker, the maximum threshold increase will be $\sim 6\text{mA}$ over the first 10 years of LHC running.

Keywords: Radiation damage, Annealing, Ageing, Laser, Optical Links, Compact Muon Solenoid, Tracker

1. INTRODUCTION

Analogue and digital optical link systems have been developed at CERN to read out and control the 10 million silicon microstrip detectors in the Compact Muon Solenoid (CMS) Tracker.¹ Most of the final link components have been chosen and the project is moving into the production phase. This follows an extensive series of validation tests of radiation hardness, functionality and reliability, in addition to a complex commercial tendering process. In this paper the series of tests, covering radiation damage, annealing and ageing, made on laser transmitters is summarized.²

Approximately 40000 lasers are required for the analogue optical readout links, in addition to 1300 lasers for the digital timing and control links. The optical link systems are illustrated in Fig. 1. The readout system transmits analogue signals from the APV readout ASICs with 8-bit resolution, at 4×10^7 samples/s. The digital system transmits both the 40MHz clock, that governs the timing of proton-proton collisions inside the experiment, as well control signals to and from the Tracker that are transmitted at 40Mbit/s. These data transmission speeds are clearly no longer at the cutting edge of optical link technology, however the large quantity of links and components, and the environmental conditions within the CMS Tracker, in particular the strong radiation field, present major challenges.

The Tracker is the closest detector system in CMS to the beam interaction point where the 7TeV proton beams of the Large Hadron Collider (LHC) will be collided. Each proton-proton collision is expected to produce ~ 100 particles and the rate of individual proton collisions will be up to $\sim 1\text{GHz}$. Many particles from these collisions pass through the Tracker causing radiation damage and, over the expected 10 year lifetime of the CMS experiment, the silicon detectors, electronics, optical links and other materials in the Tracker will be exposed to up to 2×10^{14} particles/cm² and ionizing doses up to 100kGy.³ The particle fluence at the innermost parts of the Tracker is dominated by pions and photons, with energies $\sim 300\text{MeV}$, and by $\sim 1\text{MeV}$ neutrons at the outermost modules.

* Corresponding author: karl.gill@cern.ch; telephone (+41) 22 7678583, fax (+41) 22 7672800; <http://cms-tk-opto.web.cern.ch>; CERN EP Division, CH-1211, Geneva 23, Switzerland.

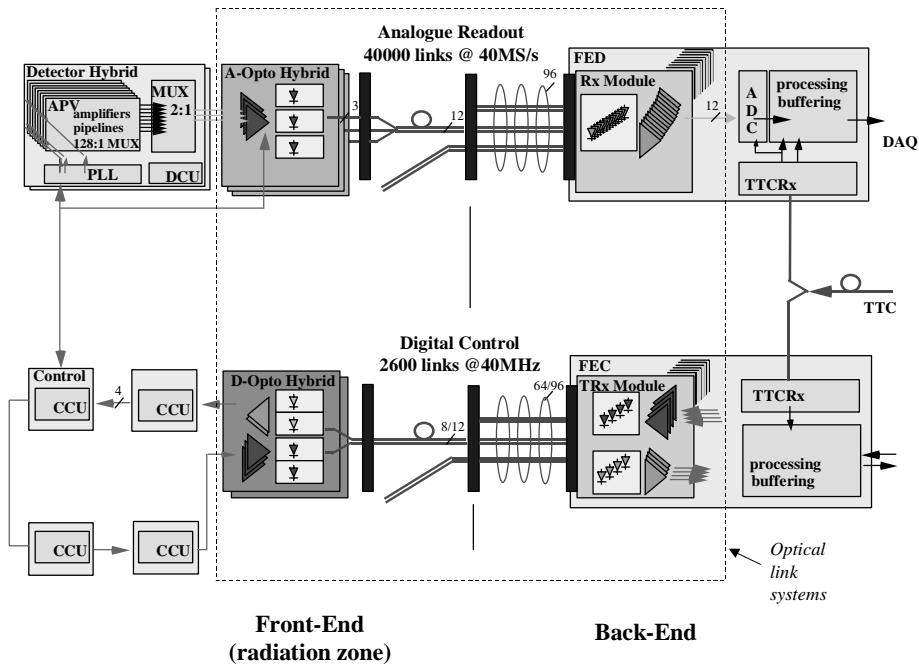


Figure 1: CMS Tracker readout and control systems. The optical link systems are highlighted in the centre of the diagram. The analogue readout links are uppermost and below these are the digital timing and control links. Components at the front-end are exposed to high levels of radiation, a 4T magnetic field and will operate at -10°C .

Given the large number of optical links in the system, it has been necessary to use commercial off-the-shelf (COTS) devices wherever possible in order to minimize the cost and the development effort. Apart from the CERN-designed ASICs at the front-end (the laser drivers and digital receivers), all of the elements are either COTS or devices based closely on COTS and, as such, these components have no guarantee of radiation hardness. Extensive testing has therefore been carried out to validate all link components situated at the front-end for use in the harsh radiation environment.⁴⁻⁹ These investigations have allowed identification of component manufacturers and suppliers that have since been invited to tender for the final supply. The test data have also allowed appropriate tailoring of the optical link specifications¹ to ensure that the system can compensate for unavoidable effects, such as those due to radiation damage, now that these effects have been quantified.

In addition to radiation damage concerns the devices must operate for at least ten years inside CMS. Manufacturer-qualified commercial off-the-shelf (COTS) components are already qualified as being highly reliable, however it is not known in advance if radiation damage influences the long-term reliability of a particular optoelectronic component. Tests of long-term degradation in pre-irradiated devices have therefore been undertaken.¹⁰

Amongst all the optical link components located inside the CMS tracker, the lasers are considered to be the most sensitive elements in terms of radiation damage and reliability. The most important long-term failure mode is likely to be linked to the increase in threshold current resulting from a combination of radiation damage and wearout degradation.^a If the threshold current I_{thr} increases, due to radiation damage and wearout, beyond the available d.c. preset bias $I_{bias(max)}$, as shown in Fig. 2, the optical signal would be truncated in amplitude. This would be considered a failure in an analogue optical link and would also eventually lead to failure in a digital optical link if the threshold current continued to increase. The analogue laser driver ASIC (re-used also at the front-end of the digital optical links) therefore includes a programmable offset dc bias current, of up to 45mA,¹¹ in order to track laser threshold changes during operation and to provide protection against this failure mode.

^a In this paper random failure mechanisms are not considered since such tests should be based upon real operational data for a large number of device-hours.

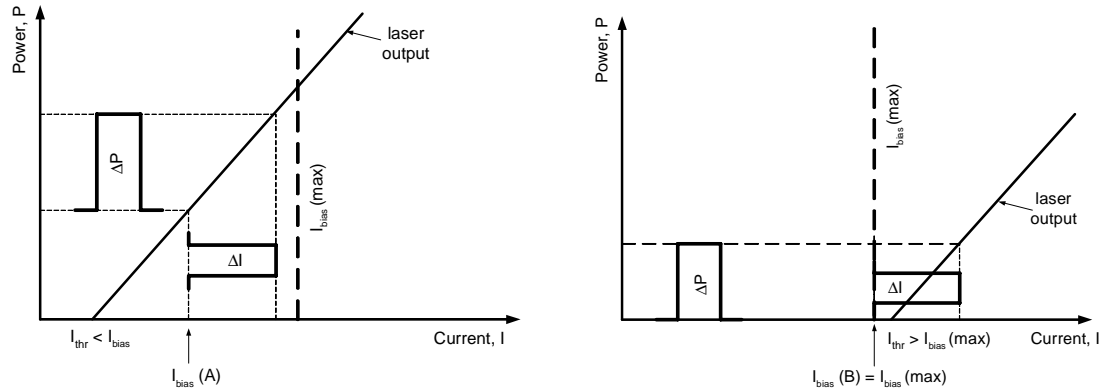


Figure 2: Two schematic laser L-I characteristics illustrating optical link failure due to the increase in laser threshold current I_{thr} . Laser A (left plot) performs within specifications whereas laser B (right plot) has failed since the threshold current has increased beyond the available dc bias current $I_{bias} (max)$ causing truncation of the output optical signal power ΔP .

Up to the point when the laser type was chosen, only a limited series of validation tests had been performed on these lasers, involving the use of ^{60}Co -gamma and $\sim 0.8\text{MeV}$ neutron sources. A primary objective has therefore been to prove that these particular lasers are indeed sufficiently radiation hard and reliable enough for the final application by making further radiation damage tests using other particle sources and by carrying out annealing and ageing studies.

In particular, the damage from pions has been investigated, since this is expected to be the most serious source of radiation damage in the Tracker. Annealing of radiation damage (from neutrons) has then been measured both as a function of bias current and temperature in order to gain further insight into the acceleration mechanisms and to understand whether there might be some means of increasing the rate of annealing within the operating parameters of the final system, e.g. by supplying a larger bias current. Devices have also been irradiated at their intended working temperature close to -10°C . Finally, some irradiated lasers have been aged at 80°C to observe whether the radiation damage has had any influence on the long-term wearout.

The full series of tests are described in the following sections along with a prediction of the expected degradation over the full lifetime for lasers at various points in the Tracker based on the combined data from the damage, annealing and wearout measurements.

2. EXPERIMENT

2.1 Lasers under test

Twenty-eight devices were used in this study. It should be noted that ~ 50 other lasers from the same batches have also been tested in a separate validation study of in-system performance. The lasers were packaged by ST in their intended final form in a very compact, non-magnetic package with a single-mode fibre pigtail. All the lasers were passed through a burn-in and test procedure before delivery to CERN. The fibre was not the final type but this did not affect the results of these tests, particularly as the pigtails were no longer than a few metres. FC/PC connectors were used although MU will be used for the final system; again this did not influence the conclusions of these tests. More importantly, there are no other components in the package, such as lenses, that could be degraded significantly by (ionizing) radiation damage. Pre-irradiation laser power output characteristics as a function of input current (usually referred to as the laser 'L-I' characteristics) are shown for 8 lasers in Fig. 3. The initial laser threshold currents were around 5mA at 20°C and the output efficiencies (out of the fibre) were $\sim 40\mu\text{W}/\text{mA}$ ($\pm 20\%$) as specified for the application.¹

In this paper the focus is more upon measurements of the laser threshold current since this particular parameter has been measured on these lasers to be degraded much more by radiation damage than, for example, the laser output efficiency or laser voltage.¹² Moreover, measurements have shown that the degradation of the efficiency by displacement damage is proportional to the threshold current damage. Similarly, the laser voltage is also directly proportional to the threshold damage, being the product of the threshold current increase and the series resistance of the laser, where the series resistance value is unchanged after irradiation for these particular lasers.¹²

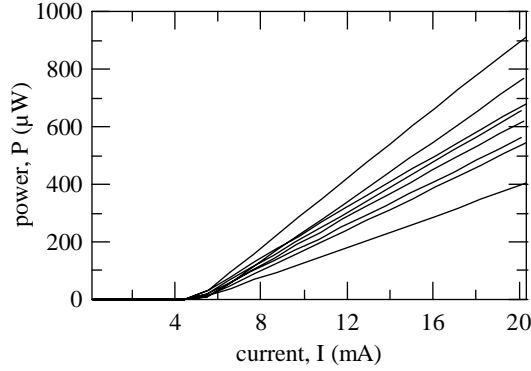


Figure 3: Typical L-I characteristics of 8 laser die packaged and supplied by ST Microelectronics.
The light power is that measured out of the fibre.

The processes governing the threshold current I_{thr} are temperature dependent and I_{thr} varies (approximately) with temperature T according to,¹³

$$I_{thr}(T_2) = I_{thr}(T_1) \exp\left[\frac{(T_2 - T_1)}{T_0}\right]. \quad (1)$$

The characteristic temperature T_0 is $\sim 60\text{K}$ for the lasers in this test, which is typical of $1.3\mu\text{m}$ InGaAsP lasers.¹³ This formula was used extensively in the data analysis in order to normalize the threshold data to a given temperature.

2.2. Irradiation, annealing and ageing procedures

The overall investigation can be divided into several stages detailed in Table 1 and summarized as follows:

Part A was focused on radiation damage study. Tests A.1 through A.4 were measurements of damage and annealing with ^{60}Co -gamma, 0.8MeV neutron, 300MeV/c pion and $\sim 20\text{MeV}$ neutron sources respectively. All these irradiations were made under similar conditions of bias and temperature in order to allow direct comparisons to be made between the tests and with previous tests made with other devices.^{4,7,8}

Part B was a measurement of the annealing following irradiation. Test B.1 investigated the effect of different forward bias settings. Test B.2 measured first of all the radiation damage at -13°C with $\sim 20\text{MeV}$ (average energy) neutrons. Then the devices were annealed at three different temperatures: 20, 40 and 60°C , with 4 lasers per temperature step. Based on the data from this test we can estimate the long-term annealing at -10°C expected in the final application.

Part C used the devices already irradiated and studied in Test B.2, and in this final set of measurements the lasers were aged at a temperature of 80°C for 2500 hours, under 60mA bias, to observe any long-term wearout degradation.

In all of these tests the lasers were connected both optically and electrically, as in Fig. 4, in order to measure the damage and annealing effects in-situ. L-I characteristics were measured at periodic intervals (10 minutes in irradiation tests shorter than 10 hours, 30 minutes in longer irradiations, and 1 hour during the ageing test). The L-I measurement was made by increasing the current in all of the lasers in steps of typically $\sim 1\text{mA}$, with the power measurement being the average of 5 readings made over a period of ~ 3 seconds at each current step. The threshold current and efficiency were then determined by fitting a line to the first 5 data points where the output power level was greater than $25\mu\text{W}$. The threshold current was defined as the point of intersection of the fitted line with the current axis and the efficiency was the slope of this line.

The irradiation sources and dosimetry methods were the following: the gamma source used in Test A.1 was the RITA facility¹⁴ at SCK-CEN. The dose rate was uniform over the devices tested and the total dose was measured using polyalanine (PAD) dosimeters attached close to the samples under test. The Prospero reactor¹⁵ at CEA Valduc for Test A.2. The neutron energy spectrum is a roughly exponential profile in energy, with an average value close to 0.8MeV. The neutron flux was maintained at a constant level throughout the irradiation. Indium foil dosimeters were placed close to the devices under test. The ionizing dose due to gamma rays emitted by the reactor was $\sim 750\text{Gy}$ per 10^{14}n/cm^2 , though based on the results of Test A, the gamma background was unlikely to have caused any significant damage. The $\pi\text{E-1}$ beam-line (detailed in Ref. 16) at PSI, was used for the pion irradiation in Test A.3. The pion momentum was selected to be 300MeV/c. The devices were positioned at the beam axis, where the width of the beam was such that the devices received the same fluence to within 10%. The accumulated fluence was measured based on the integrated signal

from an up-stream wire-chamber detector, calibrated in dosimetry runs using Al-foils of area $5 \times 5 \text{mm}^2$ placed in the same position as the samples under test. The T2 neutron irradiation facility¹⁷ of the Cyclotron Research Centre (CRC) was used for tests A.4, B and C. The neutrons are emitted with an average energy of $\sim 20 \text{MeV}$ from a beryllium target bombarded with 50MeV deuterons. Dosimetry was made by measuring the integrated deuteron beam current and comparing this with fluences measured during a previous calibration run made with a certain beam current. In all of the above cases the accuracy of the dosimetry was limited to $\sim 20\%$, due to various causes of uncertainty: statistical fluctuations, differences between the precise sample positions and dosimeter positions, as well as systematic uncertainties in activation cross-sections.

Table 1: Experimental conditions for the radiation damage, annealing and ageing studies.

Test	Number of lasers	Dose or particle fluence ($\pm 10\%$) (averaged over devices)	Irrad time (hrs)	Annealing time (hrs)	Irradiation conditions (bias and temperature)	Post-irradiation conditions (bias and temperature)	
A.1	4	100kGy ($^{60}\text{Co}-\gamma$)	46	8	Biased at 5 to 10mA above threshold, Ambient T (20-30°C)	Biased at 5 to 10mA above threshold, Ambient T (20-30°C)	
A.2	4 (same as for Test A.1)	$1.1 \times 10^{15} \text{ n/cm}^2$ (mean neutron energy = 0.8MeV)	6.5	115	Biased at 5 to 10mA above threshold, Ambient T (20-30°C)	Biased at 5 to 10mA above threshold, Ambient T (20-30°C)	
A.3	4	$1.1 \times 10^{14} \pi/\text{cm}^2$ (pion momentum = 300MeV/c)	32	120	Biased at 5 to 10mA above threshold, Ambient T (20-30°C)	Biased at 5 to 10mA above threshold, Ambient T (20-30°C)	
A.4	2	$4.2 \times 10^{14} \text{ n/cm}^2$ (mean neutron energy = 20MeV)	3.2	74	Biased at 5 to 10mA above threshold, Ambient T (20-30°C)	Biased at 5 to 10mA above threshold, Ambient T (20-30°C)	
B.1	6	As for Test A.4			Unbiased, Ambient T (20-30°C)	Biased (0,30,60mA, 2 devices per current value) Ambient T (20-30°C)	
B.2	12	up to $4.4 \times 10^{14} \text{ n/cm}^2$ (mean neutron energy = 20MeV)	3.5	16 (at -13°C) 500 (at other temperatures)	Unbiased, Cooled (-13°C)	Unbiased, Heated (T=20,40,60°C, 4 devices per T value)	
C	12 (same as for Test B.2)	As for test B.2					Test B.2, followed by ageing: T=80°C, I=60mA, t=2500 hrs

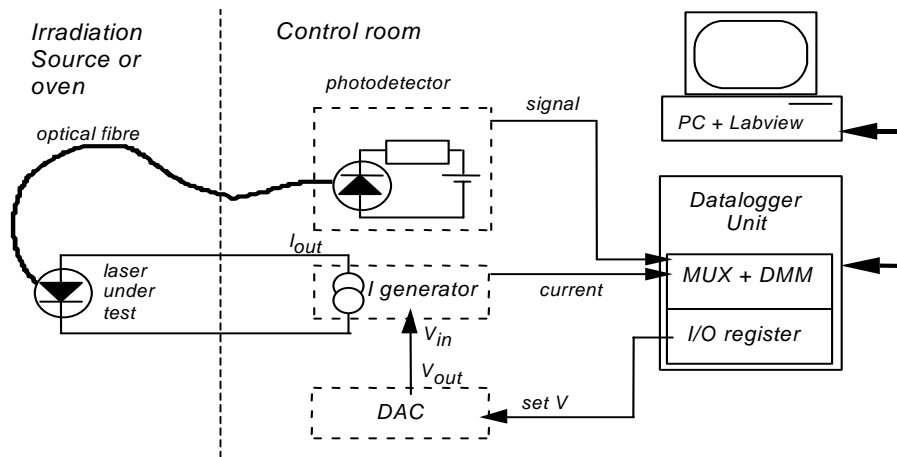


Figure 4: Control and data-acquisition system for in-situ measurement of laser L-I characteristics during irradiation or ageing. Only one laser is shown but the system was used to test many devices in parallel.

3. RESULTS

3.1 Test A: Radiation damage study

3.1.1 Test A.1: ^{60}Co gamma

The L-I characteristics measured before and after gamma irradiation are illustrated in Fig. 5, for the four lasers tested, where it is clear that irradiation to 100kGy had little effect on the light output characteristic. This result is consistent with tests on lasers from other manufacturers, where no damage was observed at the level of the laser die after gamma irradiation.¹²

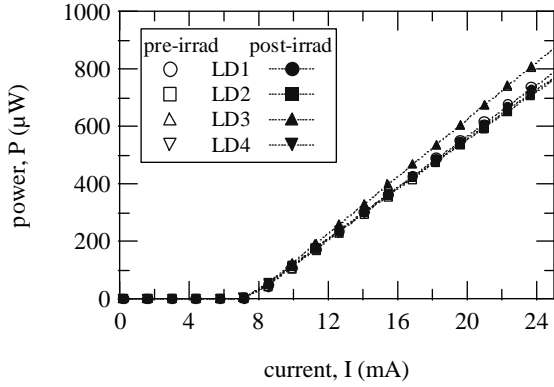


Figure 5: Laser characteristics before and after 100kGy.

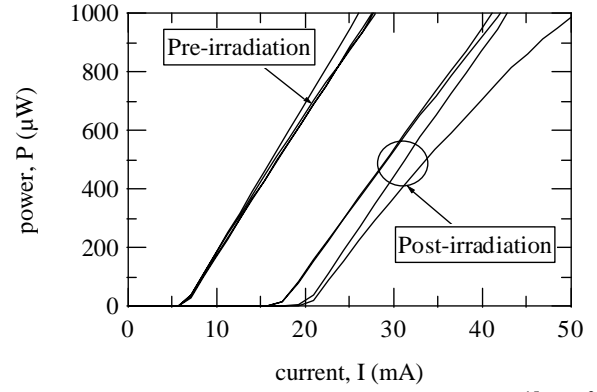
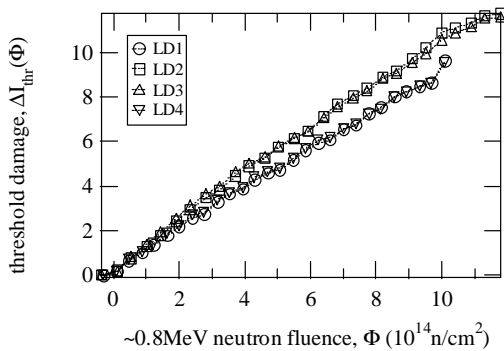


Figure 6: Laser characteristics before and after $1.0 \times 10^{15} \text{ n/cm}^2$.

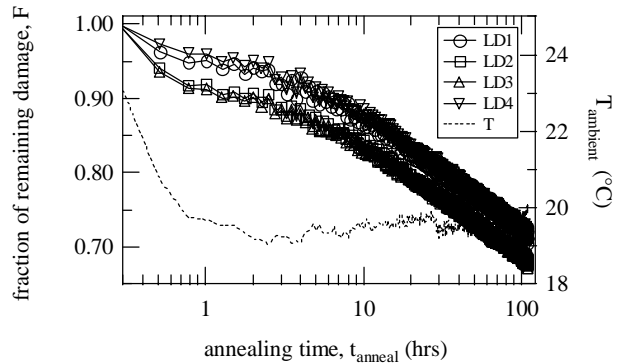
3.1.2 Test A.2: 0.8MeV neutrons

The L-I characteristics for the four lasers measured before and after neutron irradiation with the PROSPERO reactor, are illustrated in Fig. 6. These were the same lasers that were irradiated with gammas in Test A.1, and based on the findings of earlier tests⁴ it is unlikely that the pre-irradiation with gammas influenced these data for neutron damage. In contrast to the gamma irradiation there is now a clearly visible effect caused by displacement damage, with an increase of threshold current and a small decrease in efficiency. Fig. 7(a) shows the increase in threshold damage, ΔI_{thr} , versus neutron fluence for all four devices, normalized to 20°C using equation (1). The damage is almost linear with fluence, as observed in neutron damage studies of lasers from a variety of manufacturers.⁸ The total neutron fluence was $1.0 \times 10^{15} \text{ n/cm}^2$ at devices 1 and 4 and a slightly higher value of $1.2 \times 10^{15} \text{ n/cm}^2$ for devices 2 and 3. The lasers were mounted on a printed circuit board on which devices 2 and 3 were ~1cm closer to the reactor than devices 1 and 4. Fig. 7(b) shows the annealing of the threshold damage after irradiation. The data have been plotted in a normalized way as the fraction of remaining damage, F , defined as the threshold damage, $\Delta I_{thr}(t_{anneal})$, remaining after a certain annealing time divided by the threshold increase, $\Delta I_{thr}(\Phi, t_{irrad})$, measured at the end of irradiation,

$$F(t_{anneal}) = \frac{\Delta I_{thr}(t_{anneal})}{\Delta I_{thr}(\Phi, t_{irrad})} \quad (2)$$



(a)



(b)

Figure 7: (a) Laser threshold damage versus neutron fluence and (b) annealing of the damage after irradiation.

The annealing after the first ten hours is linear with $\log(\text{time})$, as in the previous annealing studies of other types of lasers (and photodiodes).⁷ The deviation from linearity just after irradiation is expected to be due to the annealing of damage that occurred already during the irradiation period.

There is a small difference in the rates of damage (and annealing just after irradiation) between the two pairs of lasers which was caused by a difference in temperature between the devices. The precise difference was unknown but LD2 and LD3 were clearly warmer than LD1 and LD4 as the former devices were closer to the reactor core. The core temperature reached $\sim 70^\circ\text{C}$ during operation and the air around it was not cooled. At the end of irradiation the temperature measured at the PT100 sensor close to the lasers was 28°C , falling to 20°C after one hour. Once the temperature was stable and uniform the damage in all the lasers annealed at the same rate, supporting the argument that the offset between the damage in the two pairs of lasers was related simply to a difference in the temperature, occurring only during the irradiation and during the first hour of annealing after irradiation.

3.1.3 Test A.3: 300MeV/c pions

Four lasers were irradiated with 300MeV/c pions at PSI up to $\sim 1.1 \times 10^{14}/\text{cm}^2$. The threshold damage versus pion fluence is plotted in Fig. 8(a). The threshold current increase has again been corrected to 20°C operation, using equation (1) and data from a PT100 resistor located near the samples. The radiation damage effects are qualitatively similar to those seen under neutron irradiation, with a roughly linear increase in threshold damage with fluence. However, it is clear that 300MeV/c pions are several times more damaging than $\sim 0.8\text{MeV}$ neutrons. A more precise comparison, taking into account the annealing that has occurred during the irradiation, is made later in Section 4.1.

Fig. 8(b) shows the annealing of the threshold damage after pion irradiation. The data is very similar for all the devices although less total (fractional) annealing was observed than in the neutron data of Test A.2 (and the later test A.4). This effect was expected since the irradiation duration of 32 hours was not much shorter than the measured annealing period of 110 hours. The annealing taking place during irradiation therefore reduced significantly the rate of annealing post-irradiation, for at least around the first 40 hours.

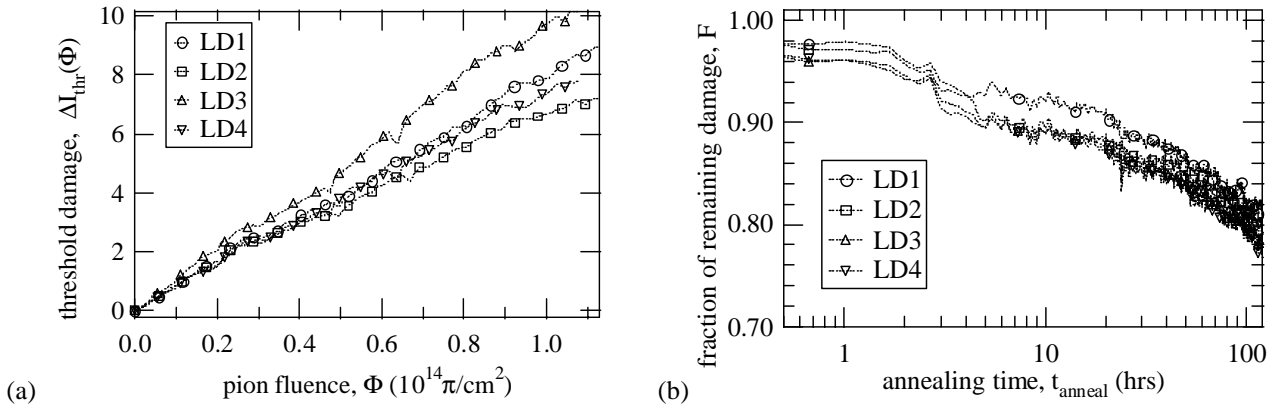


Figure 8(a): Laser threshold damage versus pion fluence and (b) annealing of the damage following irradiation.

3.1.4. Test A.4: 20MeV neutrons

Two lasers were irradiated with $4.2 \times 10^{14}/\text{cm}^2$ (20MeV average energy) neutrons at the CRC neutron source. Apart from the particle flux being different to the tests A.1, A.2 and A.3, the irradiation was made under similar conditions of bias and temperature in order to allow comparisons with the damage from the other sources.

The threshold damage versus neutron fluence is shown in Fig. 9(a) and the annealing is shown in Fig. 9(b). It is immediately clear that the $\sim 20\text{MeV}$ neutrons at CRC are much more damaging than the $\sim 0.8\text{MeV}$ neutrons at Prospero. There is a slight difference between the amounts of damage in the two devices that is difficult to explain, particularly given the limited data-set. The annealing again has a linear dependence with $\log(\text{time})$ and here the effects are almost identical in both lasers. There is a small discontinuity after 10 hours of annealing which is related to a minor problem in cooling the lasers.

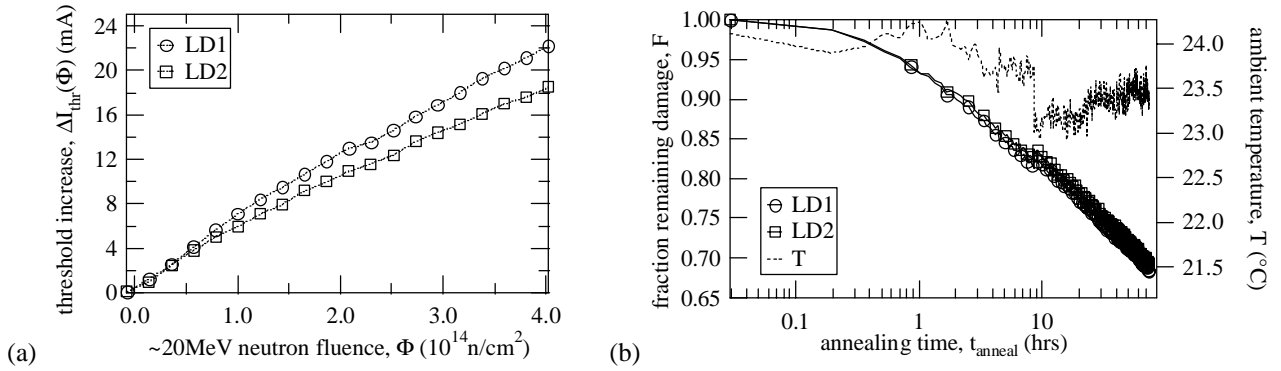


Figure 9(a) Laser threshold damage versus accumulated neutron fluence and (b) annealing following irradiation

3.2. Test B – Annealing study

3.2.1. Test B.1. Annealing versus bias current

Six lasers were irradiated to a total fluence between 4.4 and $4.7 \times 10^{14} \text{ n/cm}^2$ at the CRC neutron source alongside the devices measured in Test A.4. In between L-I characteristic measurement cycles the devices in this test were kept unbiased. Then, at the end of irradiation, the devices were biased at 0mA (LD1 and LD2), 30mA (LD3 and LD4) and 60mA (LD5 and LD6).

Fig. 10 illustrates (a) the evolution of the threshold current during irradiation and (b) the annealing of the damage after irradiation. The effect of increasing the bias current during the annealing period after irradiation was to increase the rate of annealing. Comparing the annealing data at 30mA to those at 0mA (after the first few hours of annealing) there is up to 3 times acceleration of the annealing under bias, considering the amount of time required to reach a certain degree of annealing. Comparing the 60mA data with 0mA there is an acceleration factor of between 6 and 10 in the annealing, again considering the amount of time required to reach a certain level of annealing.

Since the additional fraction of annealing that can be gained by increasing the current to 60mA is only ~15% of the initial damage it is unlikely that we will use this method of accelerating the annealing to reduce the damage in the lasers in the final system.

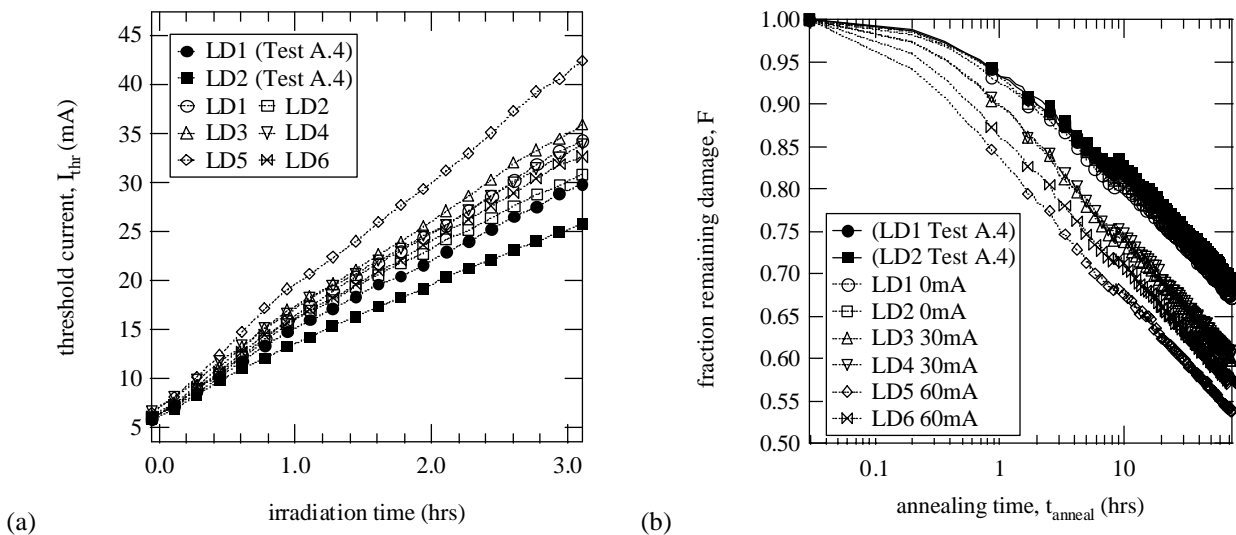


Fig. 10: (a) Laser threshold variation during neutron irradiation (LD1-6 not biased between measurements) and (b) annealing of threshold damage after neutron irradiation for different bias current values. The data from Test A.4, where devices were biased at 5 to 10mA above threshold during and after irradiation, have been included for comparison.

The data from Test A.4 were also included in these plots for comparison purposes. After taking into account the different fluences received there is more damage, in addition to greater annealing, in the Test B.1 devices. These effects can be explained by the greater amount of annealing occurring during the irradiation for the Test A.4 devices, since these devices were biased during irradiation. This reduced the amount of total damage, and in addition reduced the amount of annealing taking place just after irradiation since the short-lived defects annealed already during irradiation.

3.2.2 Test B.2: Neutron irradiation at low temperature and annealing versus temperature

In this part of the investigation 12 lasers were irradiated to between 3.5 and $4.4 \times 10^{14} / \text{cm}^2$ at the CRC $\sim 20\text{MeV}$ neutron source, at a temperature of approximately -13°C . The L-I characteristics at -13°C are shown in Fig. 11 before and immediately after irradiation. This lower temperature is close to that expected for the CMS Tracker (-10°C), therefore simulating more realistically the thermal environment of the final application. After the irradiation step, which lasted 3.5 hours, the devices were kept at -13°C for 14 hours, after which time the lasers could be removed safely from the source. The lasers were then stored in a refrigerated compartment at -35°C for up to 6 months.

The annealing study consisted of taking the devices in groups of 4 lasers, and measuring their annealing behaviour at temperatures of 20, 40 and 60°C . Fig. 12 shows (a) the threshold current before, during and up to 14hrs after the irradiation with the temperature and (b) the normalized annealing at -13°C .

The devices were kept unbiased between L-I measurement cycles to minimize the annealing during irradiation. These data can therefore be compared directly with the 0mA data from Test B.1. The threshold values before and after irradiation are lower overall than in Test B.1, due to the threshold dependence on temperature. According to equation (1), at -13°C the threshold current is a factor 1.7 lower than at 20°C . However the actual damage (per unit fluence) is about 20% greater at the lower temperature. Based on the following observations, it is likely that extra damage at -13°C occurs because of the suppression of some of the annealing that would take place in an irradiation at 20°C .

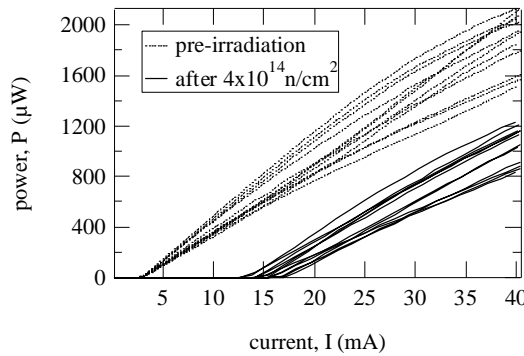


Figure 11: L-I characteristics of lasers irradiated in Test B.2.

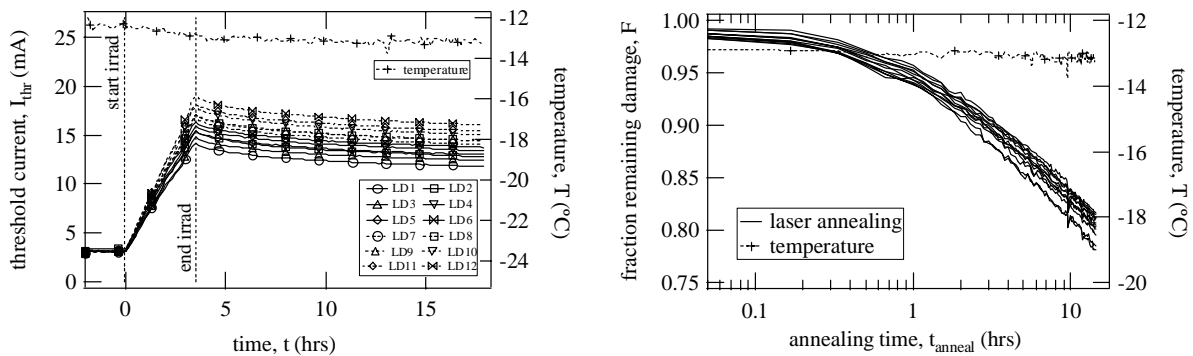


Figure 12: (a) Threshold current during Test B.2, at -13°C and (b) annealing at -13°C following irradiation.

The results for the annealing steps at the various temperatures are shown in Fig. 13. The data from one laser in the group that was annealed at 20°C was not included in this analysis since the fibre pigtail was broken during transport. The duration of each temperature step was 500 hours. The data have been normalized to the original total amount of damage measured at the end of the irradiation, i.e. the same scale as in Fig. 12(b). This was done by measuring the remaining damage at -13°C before and after each annealing step. These reference points were then used to normalize the data measured at the given annealing temperature.

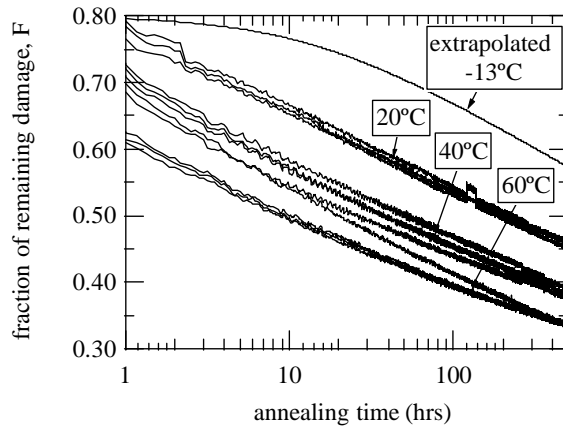


Figure 13: Annealing of laser threshold damage at various temperatures.

Also plotted in Fig. 13 is an extrapolation of the annealing at -13°C, based upon the linear dependence of annealing with log(time) that was observed towards the end of the annealing period at -13°C in Fig. 12(b). A starting point of 80% damage is assumed and a final annealing rate of 15% annealing per decade is used, consistent with that observed after irradiation. The time scale used in this extrapolation does not include the 14 hours already passed just after irradiation. This therefore allows a direct comparison with the devices that were annealed at the different temperatures (that had also previously been annealed for 14 hours at -13°C following irradiation). The lower rate at early times in the extrapolation at -13°C in Fig. 13 is simply due to the annealing that has already occurred after the irradiation (i.e. the recovery shown in Fig. 12(b)).

Further analysis is required in order to determine whether this annealing data is consistent with the annealing activation energy model that which was used in an earlier study of 1310nm lasers from another manufacturer.⁷ Nevertheless it can be concluded from this set of results that the annealing behaviour of irradiated lasers inside the CMS Tracker, at around -10°C, can be expected to continue towards very long-time periods. A similar linear dependence of annealing with log(time) is found to prevail at higher temperatures and approximately 66% of the damage is annealed at 60°C after 500 hours. It is therefore reasonable to assume that the extrapolation of the -13°C data could be extended much further, up to a point in time where the total damage remaining would be ~33% of the initial damage. This time is at around 50000 hours, which is similar to the total operational lifetime of the lasers in the CMS Tracker optical links of 10 years (or 88000 hours).

3.3. Test C – Aging at 80°C of irradiated lasers

The final step of the experimental study was the accelerated ageing for 2400 hours at 80°C of the lasers that were irradiated to $4 \times 10^{14} / \text{cm}^2$ (and then annealed) in Test B.2. L-I characteristic measurements were made at hourly intervals and the threshold current is plotted in Fig. 14.

None of the lasers exhibited any wearout-related degradation, which is typically manifested as an increase in threshold current. In this set of measurements it is clear that the annealing continued, masking the beginning of any wearout. In this test it was not possible to calculate a mean-time-to-failure (MTTF), even by extrapolation, since no degradation was observed. However, based on the Bellcore activation energy model, the 2400hr period is equivalent to a period of 10^6 hrs at -10°C, with an assumed activation energy for wearout of 0.4eV.¹⁸ During the CMS Tracker lifetime it is therefore unlikely that any lasers will fail due to an increase in threshold current caused by wearout.

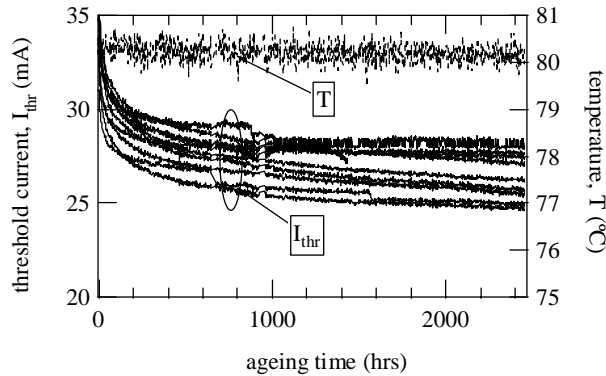


Figure 14: Laser threshold current measured during accelerated ageing step at 80°C.

4. DISCUSSION

4.1 Comparison of damage from the various sources in Tests A to D

Our previous comparisons between the damage from different sources have been made based on a 96 hour irradiation period and a total particle fluence of $5 \times 10^{14} / \text{cm}^2$.^{4,7} The new data therefore have been normalized to this fluence, whilst also taking into account the extra annealing that occurs during a longer irradiation period. The re-scaling was done by considering the effect of N consecutive irradiation steps, where $N = 96/T$ and T was the actual irradiation period (in hours). For example, thirty 3.2hr irradiation steps are combined when normalizing the data of Test A.4. The annealing of the damage introduced during the early steps is then taken into account by considering the actual annealing data measured after the irradiation period.^b

Fig. 15 compares the average damage from the radiation sources used in these tests. The displacement damage factor for neutrons of mean energy 20MeV (Test A.4, at UCL) relative to 300MeV/c pions (Test A.3, at PSI) is 0.53. The damage factor for neutrons of mean energy 0.8MeV (Test A.2, at Prospero) relative to 300MeV/c pions is 0.12. The uncertainties in these factors are $\sim 25\%$ based on the combined uncertainty from the dosimetry and the spread in the damage that was averaged over the samples used in a given test. The large difference in damage factors for 300MeV/c pions and the lower energy neutrons is expected to be related to the large difference in non-ionizing energy loss (NIEL)¹⁹ of the recoiling atoms and nuclei that are displaced following collisions between the radiation and the atoms in the crystalline bulk material of the laser. The precise NIEL values have not yet been calculated for the complicated material structure of the lasers; indeed it is not yet known whether the important displacement damage occurs in the InGaAsP or the InP regions of the laser, or at the interfaces between material boundaries. These points remain areas for further study.

For comparison with the damage factors measured here, the values obtained in a previous test of 1310nm lasers diodes from another manufacturer were 1:0.41:0.09 (300MeV/c pions : $\sim 20\text{MeV}$ neutrons : $\sim 0.8\text{MeV}$ neutrons)⁷ and more recently 1:0.67:0.12 for 1310nm InGaAsP/InP lasers from a third manufacturer (although in this latter case the uncertainty in the factors was up to $\sim 50\%$ as the devices exhibited a large spread in the amount of damage).¹² The damage factor values for these three types of laser are fairly similar, as would be expected for displacement damage in devices made from the same material. However, it is expected that the precise structure of each laser type might influence the amount of radiation damage, possibly causing some differences in the damage factors. The damage to the laser is often normalized by the starting threshold current, which is related to the detailed structure of the laser. In the future validation tests of the final lasers intended for the Tracker optical links there should be enough statistics available to be able to determine whether the threshold damage should indeed be normalized by the initial threshold value, especially if there is some variation between data from lasers originating from different wafers.

^b In the case of Test A.4 a fit and then an extrapolation of the annealing data was made in order to cover the 96hr period.

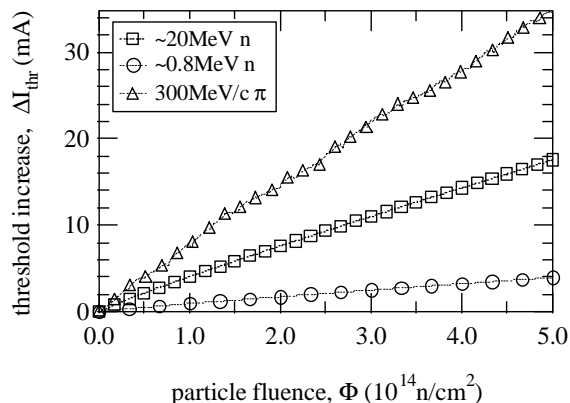


Figure 15: Average threshold current increase compared for various sources: ~ 0.8 MeV neutrons, 300 MeV/c pions, and ~ 20 MeV neutrons. The data have been averaged over the devices in each test and then normalized to a total fluence of 5×10^{14} n/cm 2 in a 96 hr irradiation period.

4.2 Prediction of damage expected in the CMS Tracker

An estimate of the damage expected in this type of laser operating in the CMS Tracker can now be made, based on the combined radiation damage and annealing measurements and some assumptions about the LHC accelerator performance and the extrapolation of the observed damage effects to long lifetimes.

There is a cocktail of particles contributing to the flux at any given point in the Tracker³ and we will make an estimation of expected damage in the lasers based on the assumption that all charged hadrons cause the same amount of damage as 300 MeV/c pions, used in Test A.3 at PSI, and that all the neutrons cause the same damage as the ~ 20 MeV neutrons used in Tests A.4, and Test B, at CRC.

The first assumption given here is justified by consideration of the laser positions at the lowest radii in the Tracker nearest the proton-beam interaction point. Here the damage will be greatest and the hadron flux is dominated by charged pions with energies around 300 MeV. Although this is higher than the energy of the pions used in PSI (where the momentum of 300 MeV/c corresponds to a kinetic energy of ~ 200 MeV), it is not expected that the non-ionizing energy loss contribution will be significantly different to 300 MeV/c pions for a given pion-nucleus collision. In fact the 300 MeV/c pions in Test A.3 probe the worst-case expected for pion damage, since this beam momentum corresponds to the largest resonant peak in the pion-nucleon interaction cross-section²⁰ and therefore the use of the data from the pion irradiation for a long-term prediction should be very conservative.

The second assumption relating to the neutron damage maintains a conservative approach to these predictions. In the outermost regions of the CMS Tracker neutrons dominate the incident particle flux, with the energy of the neutrons being ~ 1 MeV since these particles are products of spallation reactions occurring in the electromagnetic calorimeter (ECAL),³ rather than particles created at the beam-interaction point where the energy can be much larger. The CRC neutron source (~ 20 MeV) was ~ 4.4 times more damaging than the Prospero neutron source (~ 0.8 MeV), therefore using the CRC data should add an extra safety margin in the calculation of the expected damage due to neutrons in the Tracker.

A third assumption is that we can extrapolate the annealing observed in a short time at -13°C to the much longer timescales associated with the final application, as mentioned in Section 3.2.2. The results of annealing at the higher temperatures suggest that this is a good assumption for annealing of up to 65% of the damage introduced (during any given 3.5 hour irradiation period).

As a further (conservative) approximation we will assume that the annealing at -10°C will be the same as the annealing at -13°C . Even at the longest annealing times envisaged, i.e. 10 yrs, or ~ 90000 hours, the projected annealing at -10°C will only be $\sim 10\%$ more than the annealing that was experimentally observed (in the 500 hours at 60°C in Test B.2) therefore we do not extrapolate very far beyond the measured annealing. Moreover, the ageing data of Test C indicated that the annealing of the damage in the lasers would continue even further.

In these predictions the total fluence of particles is spread over a 10-year profile that allows for the expected evolution of performance of the LHC accelerator, i.e. a gradual increase of the accelerator luminosity from $0.1 \times 10^{34} \text{cm}^2 \text{s}^{-1}$ (year 1), to $0.33 \times 10^{34} \text{cm}^2 \text{s}^{-1}$ (year 2), then $0.66 \times 10^{34} \text{cm}^2 \text{s}^{-1}$ (year 3), and finally $1 \times 10^{34} \text{cm}^2 \text{s}^{-1}$ (years 4-10). Each year it is assumed that the LHC runs (with uniform luminosity) for 4 months ($\sim 2800 \text{hrs}$) before shutting down for 8 months. This is the profile that has been used in the Tracker radiation flux simulations.³

The expected time-profile of the damage that accumulates in a laser during a given year of LHC operation can then be built up from an ensemble of small irradiation steps, each 3.5 hours long. This requires 800 steps to make a total irradiation period of 2800 hrs. With this method we can make use of damage and annealing data from Test B.2. The annealing, both during and after the irradiation can also be included by summing all the remaining damage contributions from earlier irradiation steps, and by using extrapolation similar to (but further than) that made in Fig. 13 to complete the annealing for the full calendar year, i.e. up to $t=8750 \text{hrs}$. The resulting profile of incremental damage and annealing resulting from a given year of LHC operation is shown in Fig. 16(a) where 100% damage is equivalent to that introduced in 2800 hrs of LHC running. About 52% of the total damage introduced will be left at the end of the annual LHC running period and by the end of the full year, including the LHC shutdown, a further 12% of the damage will have annealed.

The profile in Fig. 16(a) describes completely the first full year of LHC running (i.e. 4 months of irradiation (and annealing), followed by 8 months of annealing). For later operating years the annealing of radiation damage introduced during earlier years also must be included. This effect is included in the full ten-year profile shown in Fig. 16(b), which also includes the effect of ramping up the LHC luminosity.

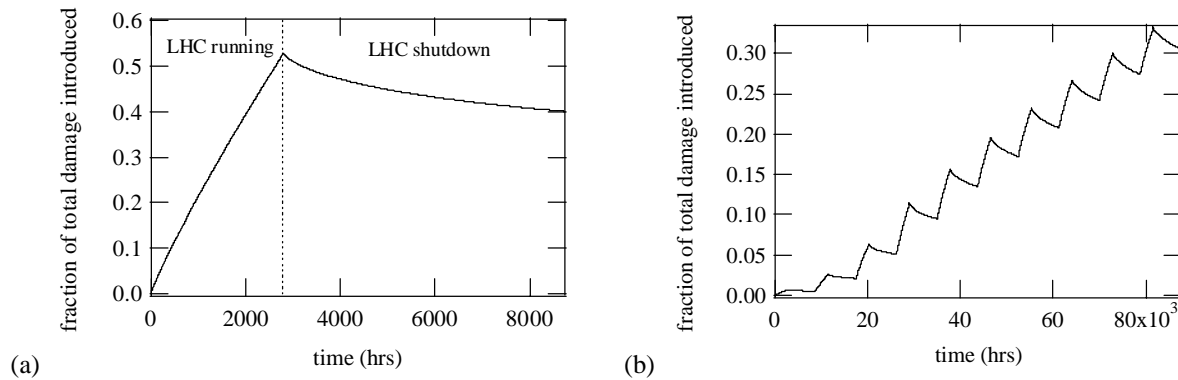


Figure 16(a): Damage and annealing profile during a year of LHC running and (b) during the first 10 years of LHC running. 100% on the y-axis refers to the entire damage introduced into the laser over the total irradiation period.

The calculation of the actual threshold increase expected for a laser in a given position in the Tracker is then straightforward based upon this profile. It is essentially the total damage measured in Test B.2, scaled to be equivalent to the appropriate cocktail of particles, and then scaled to the appropriate total fluence.

To facilitate the calculations of the total damage, the data from Test B.2 were normalized by the fluences received at each laser, with the result that for a fluence of 10^{14} ($\sim 20 \text{MeV}$ neutrons)/ cm^2 in a 3.5 hour exposure, the laser threshold current would increase by $3.4 \pm 0.1 \text{mA}$. Considering a situation where this fluence would be received over a longer period, this threshold increase represents 100% of damage introduced if the irradiation period is considered to be built up of many consecutive 3.5hr steps. For example, if a fluence of particles equivalent to 1×10^{14} ($300 \text{MeV}/c$ pions)/ cm^2 was accumulated at some position in the Tracker over the first ten years of LHC running then the total damage expected can be calculated as follows. First of all, a fluence of 10^{14} ($300 \text{MeV}/c$ pions)/ cm^2 is equivalent to 1.9×10^{14} ($\sim 20 \text{MeV}$ neutrons)/ cm^2 , according to the calculated damage factors for the PSI and CRC radiation sources. The total damage introduced into the laser, according to the convention presented here, would therefore be $1.9 \times 3.4 = 6.5 \text{mA}$. However the total visible damage, i.e. after the 10th year of LHC operation and including all the annealing up to that point, would correspond to a threshold increase of 31% of this value, according to Fig. 16(b), an increase of 2.0mA .

Table 2 summarizes the threshold increases expected at various points in the CMS Tracker. The total equivalent fluences of 300MeV/c (PSI) pions and ~20MeV neutrons (CRC) include a safety factor of 1.5, which allows some safety margin to compensate for the various systematic errors in the CMS radiation environment simulations.³ The worst-case for the optical links is given in the 2nd row of Table 2, with the total threshold increase due to accumulated radiation damage expected to be 5.3mA. It should be noted that, given this level of damage to the threshold current, it is expected that the laser efficiency will be decreased by no more than ~5%, based upon more detailed measurements of these device that are beyond the scope of this report. No additional threshold increase due to long-term wearout was included in this estimation since no degradation was observed during the accelerated ageing study (Test C).

Table 2: Laser threshold current increases expected over first 10yrs of LHC running at various points in the Tracker.

Position in Tracker (r, z) (cm)	Predicted fluence F_H (fast hadrons not including neutrons) ($10^{13}/\text{cm}^2$)	Equivalent test fluence of 300MeV/c (PSI) pions, required to validate devices for predicted fluence F_H ($10^{13}/\text{cm}^2$)	Predicted fluence F_N (fast neutrons, >100keV) ($10^{13}/\text{cm}^2$)	Equivalent test fluence of ~20MeV (UCL) required to validate devices for predicted fluence F_N ($10^{13}/\text{cm}^2$)	Predicted maximum total threshold increase (pions + neutrons = total) (mA)
r=22, z <50	12	18	3.5	5.3	3.6 + 0.6 = 4.2
r=22, z=162	15	23	4.1	6.2	4.6 + 0.7 = 5.3
r=58, z <85	1.9	2.9	1.7	2.6	0.6 + 0.3 = 0.9
r=115, z <85	0.21	0.32	1.1	1.7	0.1 + 0.2 = 0.3
r=72, z=274	1.3	1.9	3.4	5.1	0.4 + 0.5 = 0.9

5. CONCLUSIONS

A series of accelerated tests consisting of radiation damage from a variety of sources, annealing of damage, under different environmental conditions, and finally long-term ageing have been made on 1310nm InGaAsP/InP multi-quantum well lasers.

In terms of radiation damage, the lasers were not affected by ionization damage from 100kGy ⁶⁰Co irradiation, but were affected significantly by displacement damage under pion and neutron irradiation, using test fluences in excess of 10^{14} particles/cm². The 300MeV/c pions were most damaging of the sources used with the relative damage factors being ~0 : 0.12 : 0.53 : 1 for ⁶⁰Co-gamma, 0.8MeV (average energy) neutrons, 20MeV (average energy) neutrons with respect to 300MeV/c pions.

The threshold current damage anneals following irradiation with the recovery being proportional to log(annealing time). The annealing can be accelerated by either increasing the laser bias current or by increasing the temperature of the laser. Up to around 70% of the damage (introduced in 3.5hrs irradiation) was annealed in 500 hours at 60°C. The results suggest that the annealing measured at -13°C, which is close to the operating temperature of the Tracker (-10°C), can be extrapolated confidently to very long timescales, for example the first 10yrs of LHC running.

Irradiated lasers did not degrade measurably during 2500hrs ageing at 80°C at 60mA bias. Based on an assumed activation energy for wearout of 0.4eV, this suggests that the lifetime of an irradiated laser is well in excess of 10⁶hrs at -10°C for the levels of radiation damage considered here.

The precise details of the damage and annealing mechanisms are not yet understood and remain open to further study. However the essential features of the radiation damage: the linear introduction of damage with particle fluence and then the linear annealing with log(annealing time) allow a robust extrapolation of the experimental data to the long-lifetime conditions of the intended application. It was calculated that in the worst-case expected for lasers operating inside the Tracker, the damage to the threshold current will be limited to ~6mA (and the corresponding efficiency loss limited to ~5%).

It can be concluded that this type of laser is suitable for the CMS Tracker application in terms of radiation resistance and reliability. There is a large safety margin which will also allow for some tolerance of variations in radiation resistance of laser die from different wafers that will be used for final production of the links.

ACKNOWLEDGMENTS

The authors would like to thank the staff of the various irradiation facilities: Marc Decreton, Francis Berghmans, Marco Van Uffelen, Benoit Brichard, Simon Coenen and Frans Vos at SCK-CEN; Phillippe Zyromski at CEA Valduc, Guido Rycckewaert, Ghislain Gregoire, Eric Forton and Guy Berger at CRC; Kurt Gabathuler (and Maurice Glaser from CERN) at PSI. We are also grateful to Marc Tavlet and Michael Moll of CERN for their assistance with dosimetry measurements and to Christophe Sigaud and Loic Baumard of CERN for preparation of the test hardware.

REFERENCES

1. CMS tracker optical links system. <http://cms-tk-opto.web.cern.ch>
2. The laser type selected for the CMS Tracker Optical Links was a Mitsubishi Type ML7XX8 multi-quantum-well, 1310nm edge-emitting laser, supplied by ST Microelectronics in a very compact, non-magnetic custom package.
3. CMS Tracker Technical Design Report, **CERN LHCC 98-6** (1998).
4. K. Gill, C. Aguilar, V. Arbet-Engels, C. Azevedo, J. Batten, G. Cervelli, R. Grabit, F. Jensen, C. Mommaert, J. Troska and F. Vasey, "Radiation damage studies of optical link components for applications in future High Energy Physics experiments", **SPIE Vol. 3440**, *Photonics for Space Environments VI*, pp. 89-99, 1998.
5. J. Batten, K. Gill, J. Troska and F. Vasey. "Radiation tolerance of MT multi-way single-mode fibre-optic connectors to gamma and neutron irradiation", *Proceedings of 1997 RADECS Data Workshop*. 1997
6. J. Troska, J. Batten, K. Gill and F. Vasey, "Radiation effects in commercial off-the-shelf single-mode optical fibres", **SPIE Vol. 3440**, *Photonics for Space Environments VI*, pp. 112-119, 1998.
7. K. Gill, G. Cervelli, R. Grabit, F. Jensen, and F. Vasey, "Radiation damage and annealing in 1310nm InGaAsP/InP Lasers for the CMS Tracker" (and references therein), **SPIE Vol. 4134**, *Photonics for Space Environments VII*, pp. 176-184. 2000
8. K. Gill, C. Aguilar, V. Arbet-Engels, C. Azevedo, J. Batten, G. Cervelli, R. Grabit, F. Jensen, C. Mommaert, J. Troska and F. Vasey, "Comparative Study of Radiation Hardness of Optoelectronic Components for the CMS Tracker Optical Links", *Proceedings of 1998 RADECS Workshop*, pp.67-70. 1998.
9. F. Faccio, G. Berger, K. Gill, M. Huhtinen, A. Marchioro, P. Moreira, F. Vasey, "Single event upset tests of an 80-Mb/s optical receiver", *IEEE Transactions on Nuclear Science*, **Vol. 48, No. 5**, pp. 1700-1707, 2001.
10. K. Gill, C. Azevedo, J. Batten, G. Cervelli, R. Grabit, F. Jensen, J. Troska and F. Vasey, "Ageing tests of radiation damaged lasers and photodiodes for the CSM Experiment at CERN", *IEEE Transactions on Nuclear Science*, **Vol. 47, No. 3**, pp. 667-674, 2000.
11. G. Cervelli, A. Marchioro, P. Moreira and F. Vasey, "A radiation tolerant laser driver array for optical transmission in the LHC experiments", *Proceedings of 7th Workshop on Electronics for LHC Experiments*, **CERN/LHCC/2001-34**, 2001.
12. K. Gill. Unpublished data.
13. G. P. Agrawal and N. K. Dutta, "*Semiconductor Lasers*", 2nd Edition, Van Nostrand Reinhold, New York, 1993.
14. Radio Isotope Test Arrangement (RITA) facility. Contact person B. Brichard. SCK-CEN Instrumentation Department, Boeretang 200, B-2400, Belgium.
15. Prospero neutron irradiation facility. Contact person P. Zyromski, CEA Centre de Valduc, 21120 Is-sur-Tille, France.
16. P. Aarnio, M. Huhtinen, M. Pimia, K. Kaita, M. Laakso, A. Numminen, P. Ryyty, "Damage observed in silicon diodes after low energy pion irradiation", *Nuclear Instruments and Methods*, **A360**, pp.521-531, 1995.
17. 'T2 fast neutron source'. Contact person G. Berger, CRC, Chemin du Cyclotron 2, B-1348 Louvain-la-Neuve, Belgium.
18. Bellcore specification. "Reliability Assurance for Loop Optoelectronic Special Procedures and Test Methods for Lasers". **TA-NWT-983**, December 1993.
19. E. Burke, "Energy dependence of proton-induced displacement damage in silicon", *IEEE Transactions of Nuclear Science*, **Vol 33, No. 6**, pp. 1276-1281, 1986.
20. D. Groom et al, "The review of Particle Physics", *The European Physical Journal* **C15**, 1, 2000.